

A Geometrical Interpretation of Bell's Inequalities

Taylor Firman
University of Puget Sound

January 24, 2012

Abstract

Bell's Inequalities express constraints on the correlations of three random, binary variables and they can be applied to the interpretation of quantum mechanics. In an analysis of the theory behind these inequalities, this paper suggests a geometrical interpretation of Bell's Inequality in the form of a tetrahedron in "correlation space" to which correlation measurements are restricted. Using correlated photons produced through spontaneous parametric downconversion, we were able to experimentally demonstrate a set of measurements lying outside of this tetrahedron, negating the binary nature of hidden-variable theories.

1 Introduction

Quantum Mechanics is a statistical representation of nature in that we know the probability of specific physical characteristics of particles, but the particles themselves don't take on this characteristic until we objectively measure it, forcing the wavefunction to "collapse." This viewpoint generated controversy over the years and some rejected it in favor of a hidden-variable approach, stating that variables of which we are unaware determine characteristics of particles, not probabilistic wavefunctions. One example of hidden-variable theory was introduced by Einstein, Podolsky, and Rosen in 1935 through their EPR paradox, dealing with entangled particles.¹ Through this thought experiment, they reasoned that quantum mechanics either violates the principle of locality or is classified as incomplete, missing an additional element of reality to describe the system fully (i.e. a hidden variable). In response to this paradox, John S. Bell introduced numerical inequalities that restrict hidden variable systems but do not apply to quantum mechanical systems. Since this introduction, many experimental tests have demonstrated specific physical cases that violate Bell's Inequalities, therefore proving hidden-variable theories to be inaccurate descriptions of nature, and in 2002 specifically, Dietrich Dehlinger and Morgan Mitchell carried out one such experiment using correlated photons. By analyzing the theoretical implications of Bell's Inequalities, this study will introduce a graphical interpretation of these inequalities, and by replicating the experimental design of Dehlinger and Mitchell, the results will be applied within the interpretation.

2 Theoretical Context

Introduced in 1964, Bell's Inequality is a mathematical confirmation of quantum mechanics that disproves the validity of all hidden variable theories, no matter their complexity.² The theoretical context begins with a pair of correlated particles emitted from a single source, such as spin- $\frac{1}{2}$ particles or downconverted photons. Having come from a single parent source, these particles must have certain correlated characteristics such as spin or polarization, and knowing the state of one particle implies the state of the other. In our experiments, we used the process of Type-1 downconversion to produce two photons of identical polarization, so we will use this same context in the theoretical process. At either end of the source of correlated particles, detectors are placed to make some form of measurement, labeled A and B respectively. These detectors are given abstract orientations \vec{a} and \vec{b} , and in the polarization context, an example of such an orientation would be the angle of a polarizer placed in front of a detector. As mentioned, a hidden variable, which we will denote as λ , is present throughout the entire process. After the emission of the correlated particles, enough distance separates the two particles so that communication between them is impossible, enforcing the assumption of locality. Therefore, after emission, λ is set in place, and if known, it determines any measurement outcome.

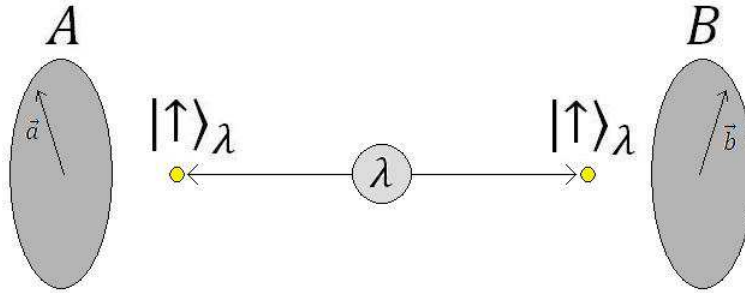


Figure 1: Theoretical set-up of photon emission towards detectors using particular orientations.

To illustrate this, consider the general case of a binary form of measurement, detection or non-detection at detector A using a single orientation \vec{a} with hidden variable λ : $A(\vec{a}, \lambda) = \pm 1$, (+1 = detection; -1 = non-detection). Since the correlated photons maintain identical polarization, any measurement at detector B using orientation \vec{a} will be identical to using \vec{a} on detector A (i.e. $A(\vec{a}, \lambda) = B(\vec{a}, \lambda)$), so in an attempt to simplify concepts, theoretical measurement notation will only use detector A .

3 Mathematical Context

To analyze the mathematical relationship between the measurements made using two different orientations in the hidden variable context, we can analyze their statistical correlation between -1 (anticorrelation) and +1 (perfect correlation). By definition, the correlation between the measurements using \vec{a} and measure-

ments using \vec{b} is

$$C(\vec{a}, \vec{b}) = \frac{\langle (A(\vec{a}, \lambda) - \mu_{\vec{a}})(A(\vec{b}, \lambda) - \mu_{\vec{b}}) \rangle}{\sigma_{\vec{a}}\sigma_{\vec{b}}} \quad (1)$$

with μ_a, μ_b being the average values of $A(\vec{a}, \lambda)$ and $A(\vec{b}, \lambda)$ respectively, and σ_a, σ_b being the standard deviation of $A(\vec{a}, \lambda)$ and $A(\vec{b}, \lambda)$ respectively. However, since we are assuming uniform probability distribution for $A(\vec{a}, \lambda)$ and $A(\vec{b}, \lambda)$ and they can only take on values of ± 1 , $\mu_{\vec{a}} = \mu_{\vec{b}} = 0$ and $\sigma_{\vec{a}} = \sigma_{\vec{b}} = 1$. This simplifies our correlation calculation down to

$$C(\vec{a}, \vec{b}) = \langle A(\vec{a}, \lambda)A(\vec{b}, \lambda) \rangle, \quad (2)$$

the expectation value of the product of the two measurements.

Since one orientation gives us a measurement and two produce a correlation, Bell's Inequality takes the next logical step by using three orientations, \vec{a} , \vec{b} , and \vec{c} , to develop a mathematical relationship between correlations. Knowing that each of the three measurements using \vec{a} , \vec{b} , and \vec{c} only have two possibilities (± 1), this leaves us with eight possible outcomes of all three measurements:

λ	$A(\vec{a}, \lambda)$	$A(\vec{b}, \lambda)$	$A(\vec{c}, \lambda)$	P_λ
1	+1	+1	+1	P_1
2	+1	+1	-1	P_2
3	+1	-1	+1	P_3
4	+1	-1	-1	P_4
5	-1	+1	+1	P_5
6	-1	+1	-1	P_6
7	-1	-1	+1	P_7
8	-1	-1	-1	P_8

Table 1: Possible measurement outcomes using orientations \vec{a} , \vec{b} , and \vec{c} , along with associated λ index and probability.

By associating each possible outcome with a hidden variable index, λ , between 1 and 8, and a probability of occurring, P_λ , we can express the expectation value of the products of various measurements by using the summation notation of

$$C(\vec{a}, \vec{b}) = \sum_{\lambda=1}^8 [P_\lambda A(\vec{a}, \lambda)A(\vec{b}, \lambda)]. \quad (3)$$

To relate these values to one another, we can take the difference of two correlations using three orientations,

$$C(\vec{a}, \vec{b}) - C(\vec{a}, \vec{c}) = \sum_{\lambda=1}^8 [P_\lambda A(\vec{a}, \lambda) (A(\vec{b}, \lambda) - A(\vec{c}, \lambda))], \quad (4)$$

and since $A(\vec{b}, \lambda)^2 = 1$,

$$C(\vec{a}, \vec{b}) - C(\vec{a}, \vec{c}) = \sum_{\lambda=1}^8 \left[P_{\lambda} A(\vec{a}, \lambda) A(\vec{b}, \lambda) \left(1 - A(\vec{b}, \lambda) A(\vec{c}, \lambda) \right) \right]. \quad (5)$$

From here, we can take the absolute value of both sides of the equation and use the triangle inequality to produce the fact that

$$|C(\vec{a}, \vec{b}) - C(\vec{a}, \vec{c})| \leq \sum_{\lambda=1}^8 \left[|P_{\lambda}| |A(\vec{a}, \lambda) A(\vec{b}, \lambda)| |1 - A(\vec{b}, \lambda) A(\vec{c}, \lambda)| \right]. \quad (6)$$

However, certain facts can simplify this relation. Since probability is always non-negative, $|P_{\lambda}| = P_{\lambda}$, and since $A(\vec{a}, \lambda) A(\vec{b}, \lambda) = \pm 1$, $|A(\vec{a}, \lambda) A(\vec{b}, \lambda)| = 1$. Furthermore, the relation $1 - A(\vec{b}, \lambda) A(\vec{c}, \lambda)$ can equal either 2 or 0, but in either case, the result is greater than or equal to 0 and therefore, $|1 - A(\vec{b}, \lambda) A(\vec{c}, \lambda)| = 1 - A(\vec{b}, \lambda) A(\vec{c}, \lambda)$. These assumptions lead to the simplified relation that

$$|C(\vec{a}, \vec{b}) - C(\vec{a}, \vec{c})| \leq \sum_{\lambda=1}^8 \left[P_{\lambda} \left(1 - A(\vec{b}, \lambda) A(\vec{c}, \lambda) \right) \right]. \quad (7)$$

Finally, we can distribute P_{λ} and split the summation to produce

$$|C(\vec{a}, \vec{b}) - C(\vec{a}, \vec{c})| \leq \sum_{\lambda=1}^8 [P_{\lambda}] - \sum_{\lambda=1}^8 \left[P_{\lambda} A(\vec{b}, \lambda) A(\vec{c}, \lambda) \right]. \quad (8)$$

Assuming normalized probability (i.e. $\sum_{\lambda=1}^8 [P_{\lambda}] = 1$) and using our definition of correlation from equation (3), this finally leaves us with Bell's Inequality,

$$|C(\vec{a}, \vec{b}) - C(\vec{a}, \vec{c})| \leq 1 - C(\vec{b}, \vec{c}). \quad (9)$$

Having directly derived this calculation from hidden variable assumptions, we know that all possible hidden variable theories must obey Bell's Inequality, so in order to disprove all hidden variable theories, one must experimentally find a violation of Bell's Inequality. Most physicists in the past have analyzed this relation as a purely mathematical one, but a graphical approach produces an interesting relation. By alternating the signs of the three correlations, we can produce four inequalities from our original one, and by associating $C(\vec{a}, \vec{b})$ with the x -axis, $C(\vec{a}, \vec{c})$ with the y -axis, and $C(\vec{b}, \vec{c})$ with the z -axis to construct a "correlation-space," the intersection of these four inequalities form a tetrahedron, as seen in Figure 2.

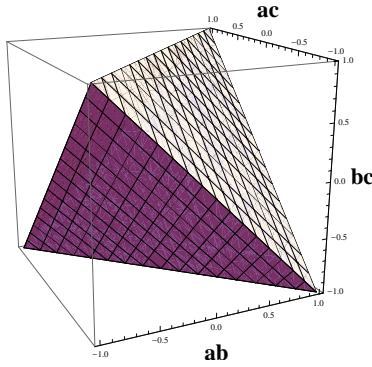


Figure 2: Tetrahedron representing all possible hidden variable correlations.

All possible correlation values in a hidden-variable context must lie within this tetrahedron and finding a violation of Bell's Inequality boils down to finding a point outside of this tetrahedron.

4 Experimental Application

In 1969, Clauser, Horne, Shimony, and Holt (CHSH) proposed an experimentally realistic version of Bell's Inequality³ by introducing a fourth orientation, \vec{b}' , to estimate $C(\vec{b}, \vec{c})$ using the relation that

$$C(\vec{b}, \vec{c}) \geq C(\vec{b}', \vec{c}) + C(\vec{b}', \vec{b}) - 1. \quad (10)$$

Theoretically, we assumed that orientation \vec{a} would produce the same result on either detector (i.e. $C(\vec{a}, \vec{b}) = C(\vec{b}, \vec{a})$), but in an experimental setting, this is unrealistic. The polarizer angle of 45° on one detector may not produce the exact same effect as 45° on the other. This relation and the fourth orientation associated with it enable us to isolate certain orientations to specific detectors: \vec{a}, \vec{b}' to detector A , and \vec{b}, \vec{c} to detector B . Originally, this estimation was used to create a purely mathematical relation of four orientations,

$$|C(\vec{a}, \vec{b}) - C(\vec{a}, \vec{c})| + C(\vec{b}', \vec{b}) + C(\vec{b}', \vec{c}) \leq 2, \quad (11)$$

but for the more intuitive graphical approach, we will use equation (10) to estimate $C(\vec{b}, \vec{c})$ as our final z -component.

At the time of the initial introduction of Bell's Inequality and the CHSH inequality, optical technology was not advanced enough to establish a clear violation. However, as time passed and technology improved, conclusive experiments began to show up, notably that of Alain Aspect,⁴ and in 2002, Dietrich Dehlinger and Morgan W. Mitchell performed one such experiment using correlated photons.⁵ Our experimental work was based on their experimental set-up as follows.

Initially, 402 nm photons just within the visible blue range are produced by a diode laser. To ensure

uniform polarization and wavelength, the beam passes through a linear polarizer and a blue filter. A pair of lenses then collimates the beam into a small point and a rotatable quartz plate introduces a phase shift to the incoming light. Next, the photons pass through a pair of birefringent Beta-Barium-Borate (BBO) crystals to undergo what is known as spontaneous parametric down conversion. In this process, the input or “pump” photon is converted into two separate photons, the “signal” and “idler” photons. Each photon obtains half of the energy of the pump photon (804 nm wavelengths) and the polarization of both photons is perpendicular to that of the pump. In accordance with the conservation of momentum, our downconverted photons veer off at an angle of $\pm 3^\circ$ with relation to the original beam. At the end of these paths, photons are passed through red filters and focused onto two avalanche photo diodes (APD) to monitor coinciding detections of these photons, ensuring the consideration of only downconverted light. Furthermore, the optical paths are enclosed in a box of opaque material and measurements are taken in complete darkness. The output of the APD’s is then passed through a wire delay and sent to a time-to-amplitude converter (TAC). A multichannel analyzer interprets the output of the TAC and finally displays a graph showing registered photon detections versus the time delay between the two detections. A noticeable peak should be located at the time of the wire delay and these detections can be counted as downconverted pairs.

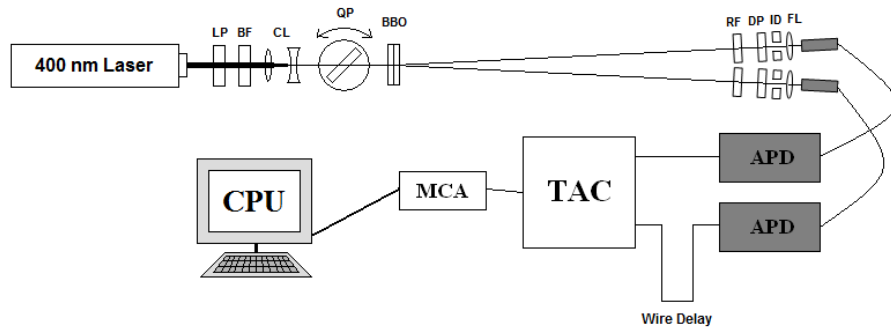


Figure 3: Theoretical diagram of experimental set-up. (LP=Laser Polarizer, BF=Blue Filter, CL=Collimating Lenses, QP=Quartz Plate, BBO=BBO Crystal, RF=Red Filter, DP=Detector Polarizer, ID=Iris Diaphragm, FL=Focusing Lens, APD=Avalanche Photodiode, TAC=Time-to-Amplitude Converter, MCA=Multichannel Analyzer, CPU=Desktop Computer)

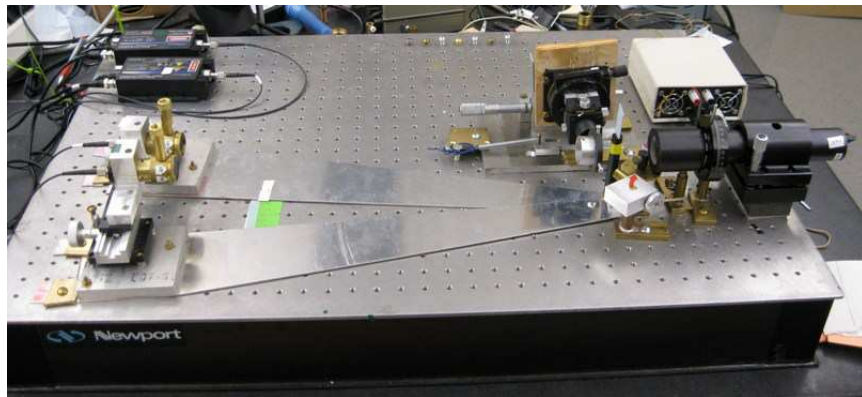


Figure 4: Actual experimental set-up. (Photograph by the author)

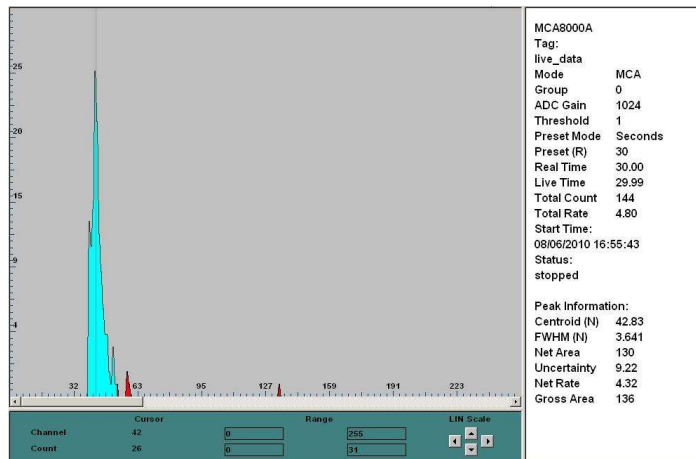


Figure 5: Sample TAC readout of photon pair detections versus the time delay between the two detections. As you can see, the greater percentage of coincidences occur in the general area of the time delay of the wire path. The units of the x -axis are the counting bins contained within the Time-to-Amplitude Converter (TAC) and are scaled based on the specific settings of the TAC.

To incorporate the abstract orientation, \vec{a} , from earlier theory, rotatable linear polarizers are placed in front of the detectors and the angles of these polarizers represent the orientation. Going back to our previous definition of correlation in equation (3), we noted that

$$C(\vec{a}, \vec{b}) = \sum_{\lambda=1}^8 \left[P_{\lambda} A(\vec{a}, \lambda) A(\vec{b}, \lambda) \right].$$

As mentioned earlier, $A(\vec{a}, \lambda) A(\vec{b}, \lambda)$ has two possible values: $+1$, corresponding to both photons passing through the polarizers and being detected or both being annihilated by the polarizers and not detected; and -1 , corresponding to only one photon passing through its polarizer and being detected. In order to count non-detected pairs, we know that anything detected at an orientation orthogonal to \vec{a} would not be detected using \vec{a} itself. By this logic,

$$C(\vec{a}, \vec{b}) = P_{ab} + P_{a_{\perp} b_{\perp}} - P_{ab_{\perp}} - P_{a_{\perp} b} \quad (12)$$

with \vec{a}_{\perp} and \vec{b}_{\perp} representing orientations orthogonal to \vec{a} and \vec{b} respectively, and P_{ab} representing the probability of detection using orientations \vec{a} and \vec{b} . Since these orientations are the only possibilities, we can calculate the probabilities by dividing the amount of coincident detections using specific orientations by the total amount of coincidences, thus making the correlation measurement

$$C(\vec{a}, \vec{b}) = \frac{N_{ab} + N_{a_{\perp} b_{\perp}} - N_{ab_{\perp}} - N_{a_{\perp} b}}{N_{ab} + N_{a_{\perp} b_{\perp}} + N_{ab_{\perp}} + N_{a_{\perp} b}}, \quad (13)$$

with N_{ab} being the number of photon coincidences detected using orientations \vec{a} and \vec{b} .

With this experimental method in place, it is also necessary to optimize our laboratory equipment to generate the largest violation of Bell's Inequality. Firstly, the polarizer immediately after the laser must be adjusted so as to balance the coincidence counts using detector polarizer angles of 0° , 0° and 90° , 90° .

Theoretically, the orientation of the laser polarizer should be oriented somewhere close to 45° . Secondly, the quartz plate must be adjusted to counteract the birefringence of the BBO crystal so as to maximize the coincidence counts using detector polarizer angles of 45° , 45° . This orientation is more sensitive and may change depending on specific laboratory conditions such as the thickness of the quartz plate and BBO crystals.

5 Results and Conclusion

In order to produce the largest theoretical violation of Bell's Inequality, the four optimal detector polarizer orientations are $\vec{a} = -45^\circ$, $\vec{b} = -22.5^\circ$, $\vec{b}' = 0^\circ$, and $\vec{c} = 22.5^\circ$, as seen in Figure 5.

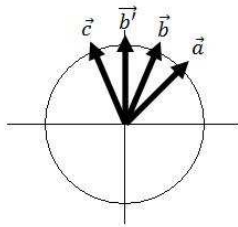


Figure 5: Optimal detector polarizer orientations ($\vec{a} = -45^\circ$, $\vec{b} = -22.5^\circ$, $\vec{b}' = 0^\circ$, $\vec{c} = 22.5^\circ$).

Using these orientations, the best calibrated run was able to produce correlations of $C(\vec{a}, \vec{b}) = 0.743$, $C(\vec{a}, \vec{c}) = -0.622$, $C(\vec{b}', \vec{b}) = 0.622$, and $C(\vec{b}', \vec{c}) = 0.742$. Typical runs did not deviate far from these values, but this optimal example best illustrates the suggested concept. Placing these values in the CHSH inequality of equation (11), one can observe a large violation in that

$$0.743 - (-0.622) + 0.622 + 0.742 = 2.729 \not\leq 2, \quad (14)$$

and with an experimental uncertainty of $\sigma = \pm 0.596$, this violates the inequality by an entire standard deviation. Furthermore, we can use equation (10) to approximate a value of $C(\vec{b}, \vec{c}) \geq 0.364$. Using these values in equation (9), Bell's Inequality itself is violated in that

$$|0.743 - (-0.622)| \not\leq 1 - 0.364 \quad \Rightarrow \quad 1.365 \not\leq 0.636, \quad (15)$$

but more importantly, if $C(\vec{a}, \vec{b})$, $C(\vec{a}, \vec{c})$, and $C(\vec{b}, \vec{c})$ are used as spatial coordinates in correlation space, the point plotted lies outside of the hidden-variable tetrahedron as seen in Figure 6.

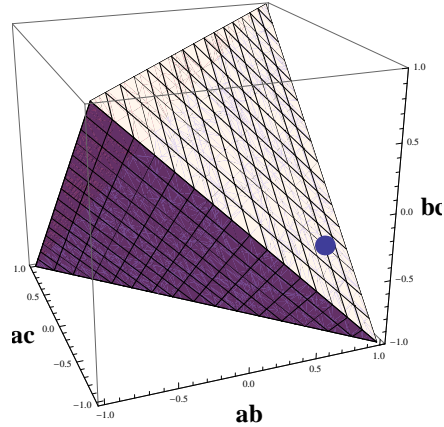


Figure 6: Graphical breach of Bell's Inequality, the set of correlations lies outside of the hidden-variable tetrahedron ($C(\vec{a}, \vec{b}) = 0.743$, $C(\vec{a}, \vec{c}) = -0.622$, and $C(\vec{b}, \vec{c}) = 0.364$).

Having established these experimental violations, one can conclusively dismiss all hidden-variable theories as improper representations of nature due to their inability to predict every possible outcome. Where quantum mechanical interpretations escape this fate is in the fact that they do not necessarily have to abide by the assumption of locality. In theory, photons randomly choose a polarization based on the probability distribution dictated by their wavefunction, but only when they are measured at the detector polarizers. In order to maintain their identical polarization, they are somehow able to affect each other instantaneously even after gaining enough separation to negate locality, a perfect example of quantum entanglement. This “spooky action at a distance,”⁶ as famously put by Einstein, would appear to violate causality, a crucial principle in the physical world, but the random nature of the effect disallows any form of communication, therefore preserving causality. While our experimental results do not explicitly confirm quantum mechanical interpretations themselves, it does reinforce them by eliminating the possibility of hidden variables.

Acknowledgments

A special thanks goes out to Alan Thorndike for his guidance in this project among many others throughout my undergraduate career. I would like to thank the University of Puget Sound, for initially sponsoring this research, as well as the many people who proofread this document. Finally, I would like to thank the Journal of Undergraduate Research in Physics for this opportunity and all of their help throughout this process.

References

- [1] A. Einstein, B. Podolsky, and N. Rosen, *Can Quantum Mechanical Description of Physical Reality Be Considered Complete?* Phys. Rev. **47**, 777-780 (1935).
- [2] J.S. Bell, *On the Einstein Podolsky Rosen Paradox*, Phys. (N.Y.) **1**, 195-200 (1964).
- [3] J.F. Clauser, M.A. Horne, and A. Shimony, R.A. Holt, *Proposed Experiment to Test Local Hidden-Variable Theories*, Phys. Rev. Lett. **23** (15), 880-884 (1969).
- [4] A. Aspect, P. Grangier, and G. Roger, *Experimental Tests of Realistic Local Theories via Bell's Theorem*, Phys. Rev. Lett. **47** (7), 460-463 (1981).

- [5] D. Dehlinger and M.W. Mitchell, *Entangled Photons, Nonlocality, and Bell Inequalities in the Undergraduate Laboratory*, Am. J. Phys. **70** (9), 903-910 (2002).
- [6] M. Born and A. Einstein, *The Born-Einstein Letters: The Correspondence Between Albert Einstein and Max and Hedwig Born, 1920-1955* (Walker, New York, 1971), pp. 157-160.
- [7] J.S. Bell, *On the Problem of Hidden Variables in Quantum Mechanics*, Rev. Mod. Phys. **38** (3), 447-452 (1966).
- [8] P.G. Kwiat, K. Mattle, H. Weinfurter, and A. Zeilinger, *New High-Intensity Source of Polarization-Entangled Photon Pairs*, Phys. Rev. Lett. **75** (24), 4337-4341 (1995).